

Riser fluctuations and vortices at Shapiro steps in Josephson-junction arrays

P. L. Leath and Y. Cai

Department of Physics and Astronomy, Rutgers–The State University, Piscataway, New Jersey 08855-0849

(Received 9 December 1994)

Numerical simulations of the giant Shapiro steps on two-dimensional arrays of resistively shunted Josephson junctions were performed at nonzero but low temperatures. When an ac current at frequency ω is applied, large phase fluctuations occur just at the risers of the Shapiro steps where the system is making the transition to the next harmonic of the applied ac current. These phase fluctuations lead to the creation of large numbers of vortices just on the risers and a large increase in noise output.

Anomalous noise-rise phenomena which cannot be explained as ordinary thermal noise have been reported in a number of experiments on Josephson-junction oscillators.^{1,2} Explanations of this noise rise for single junctions have been given by Huberman *et al.*,³ Kautz,⁴ and Pedersen and Davidson.⁵ These explanations involved the numerical calculations of the solutions to the Josephson equation of motion for a single junction in the Stewart-McCumber model,⁶ namely,

$$\beta \frac{d^2 \phi}{dt^2} + \frac{d\phi}{dt} + \sin(\phi) = i_{dc} + i_{ac} \sin(\omega t), \quad (1)$$

where ϕ is the superconducting phase difference across the junctions, $\beta = 2eJR^2C/\hbar$ with J being the critical current, R is the normal resistance, C is the capacitance of the Josephson junction, i_{dc} is the dc bias current, and i_{ac} is the amplitude of the ac applied current across the junction. These currents are measured in units of J . Here the time t is measured in units of $\hbar(2eRJ)$ and the applied frequency ω in units of $(2CRJ/\hbar)$. The voltage across the junction is given in these units by $d\phi/dt$. Huberman *et al.*³ and others found that when the capacitive term was present chaotic solutions appeared at the risers of the Shapiro steps as the junction was making the transition between the different harmonics or oscillatory states represented by the Shapiro steps. A clear analytic calculation of the origin of these effects is given by Chiao *et al.*¹ who consider the small perturbations about the limit-cycle, phase-locked solutions of Eq. (1). They consider solutions of the form

$$\phi(t) = \phi_0(t) + \phi_1(t), \quad (2)$$

where $\phi_0(t+nT) = \phi_0$ is a phase-locked solution, with $T = 2\pi/\omega$, and where the small perturbation $\phi_1(t)$ is given by

$$\phi_1(nT) = \phi_1(0)e^{-nAT}, \quad (3)$$

with

$$A = \frac{1}{T} \int_0^T \cos \phi_0(t) dt = \langle \cos \phi_0 \rangle. \quad (4)$$

For stable limit-cycle solutions $-1 \leq A \leq 1$ must be positive, as it is on the Shapiro steps. But on the riser, as the system is shifting from one limit cycle or harmonic to the

next, A must cross through zero to get to the next stable solution. When A crosses through zero, there are ac induced nulls in the supercurrent and a great increase in the noise produced, which leads to the chaotic solutions, reported by Huberman *et al.*³ We note that the presence of the capacitive term in Eq. (1) was essential for the existence of the chaotic solutions otherwise the system goes sharply from one harmonic to the next.

We report here results for $N \times N$ arrays of *resistively shunted* Josephson junctions (RSJ) at finite temperatures. The capacitance of the junction is zero but temperature fluctuations and their coupling into an array are sufficient to create a great increase in the noise on the risers of the giant Shapiro steps coupled with the emission of large numbers of vortex-antivortex pairs on each Shapiro-step riser.

The model that is used for the numerical calculations is essentially the same as that in our previous report on the below-gap photoresponse of RSJ arrays.⁷ We consider an $N \times N$ array of RSJ junctions as illustrated in Fig. 1 for $N = 6$ [the grains in the left column are connected by junctions (not shown) to those on the right column]. The external current is applied to the array by injecting it at a single superconducting grain at the top of the sample (which acts as a busbar) and removing it from a similar grain at the bottom. At each node of the $N \times N$ square array four junctions come together so that the equations of motion for each of the single junctions are added to conserve total current at the node. The resulting set of coupled equations at node K is

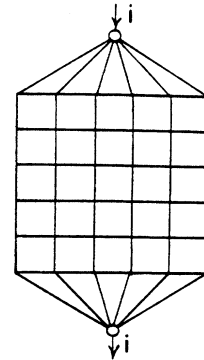


FIG. 1. A perfect 6×6 array of resistively shunted Josephson junctions connected to single superconducting grains at the top and bottom of the array, which acts as busbars. With the periodic boundary conditions the grains on the left are connected (by junctions not shown) to those on the right.

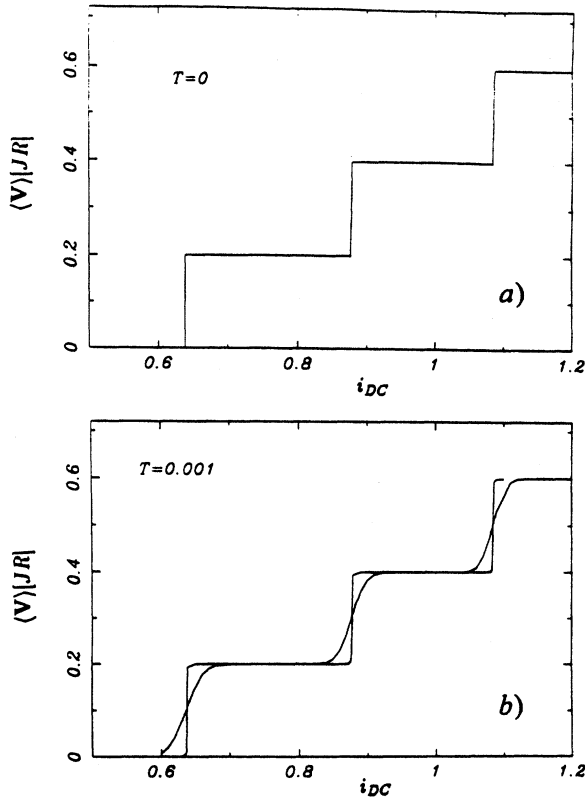


FIG. 2. The average voltage per bond $\langle v \rangle$ vs i_{dc} for a 16×16 array with $i_{ac}=0.5$, $\omega=0.2$ and (a) $T=0$ and (b) $T=0.001$. The more rounded curve in (b) is for a single junction.

$$\sum_l \frac{d}{dt} (\phi_k - \phi_l) = i_k^{ext} - \sum_l [\sin(\phi_k - \phi_l) + \tilde{i}_{kl}(t)], \quad (5)$$

where ϕ_k is the superconducting phase at node k , where the capacitive terms have been ignored, where i_k^{ext} is the external applied current

$$i^{ext} = i_{dc} + i_{ac} \sin(\omega t), \quad (6)$$

which is zero everywhere except at the top and bottom busbar, where the external current is inserted and withdrawn, and where $\tilde{i}_{kl}(t)$ is the randomly fluctuating noise current across the junction connecting nodes k and l which represents the thermal fluctuations, and is approximated by the white-noise form of Ambegaokar and Halperin⁸ with the following characteristics:

$$\langle \tilde{i}_{ij} \rangle = 0, \quad (7)$$

and

$$\langle \tilde{i}_{ij}(t + \tau) \tilde{i}_{kl}(t) \rangle = \frac{2k_B T}{J^2 R_{ij}} \delta(t) \delta_{ij;kl}, \quad (8)$$

where $\langle \rangle$ denotes an ensemble average. The noise currents in the different shunt resistances are uncorrelated, and the noise current in a single junction is uncorrelated in time corresponding to white noise (Johnson noise). These equations of motion (4) can be collectively written in the generalized matrix form

$$M \frac{d\phi}{dt} = C(\phi), \quad (9)$$

where $C(\phi)$ is the nonlinear term which includes the $\sin(\phi_k - \phi_l)$ terms of Eq. (5). These equations are solved numerically by inverting M to the right-hand side of Eq. (9) and integrating numerically, while randomly applying a different white-noise current $\tilde{i}_{kl}(t)$ to each junction in each time step. The numerical results for a single junction and 16×16 arrays of identical RSJ junctions are shown in Fig. 2. Figure 2(a) shows the Shapiro steps for both the voltage across a single junction and for the voltage across each junction in an array which coincides at $T=0$ and the voltage steps sharply between the various harmonics. On the first step the entire $N \times N$ array is phase locked to the applied ac driving current. On the n th step the system is phase locked to the $(n-1)$ th harmonic of the driving current. In Fig. 2(b), temperature fluctuations have been introduced (as current

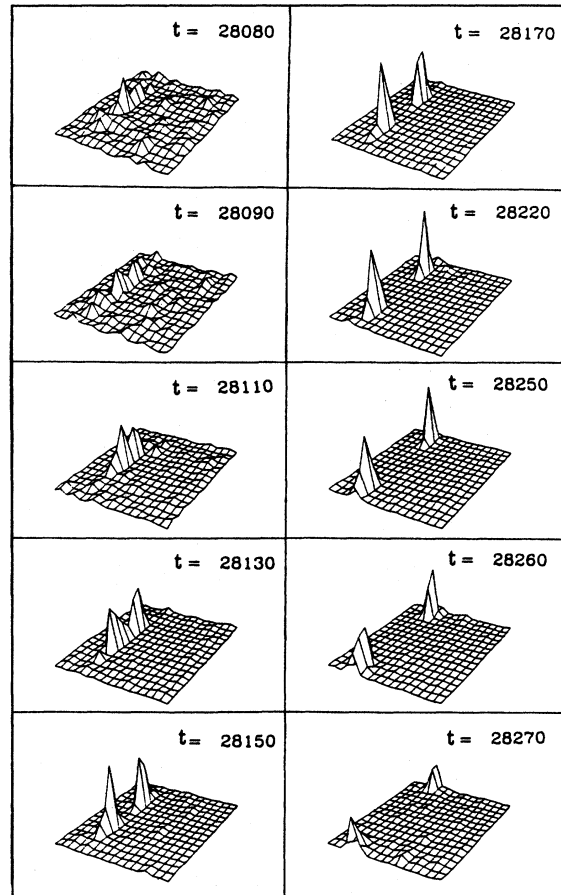


FIG. 3. Snapshots of the creation and annihilation of a vortex-antivortex pair in a perfect 16×16 array at $T=0.25$, $i_{dc}=0.7$, $i_{ac}=0.25$, and $f=0.2$. The Monte Carlo time steps are indicated on each picture as the temperature fluctuations produce a barrier to the supercurrent flow which causes the vortex and antivortex to be produced on each end of the fluctuation, to deepen, and to travel across the sample annihilating at the periodic boundary conditions. The actual plot is of the magnitude of the supercurrent flowing in the bonds perpendicular to the external current.

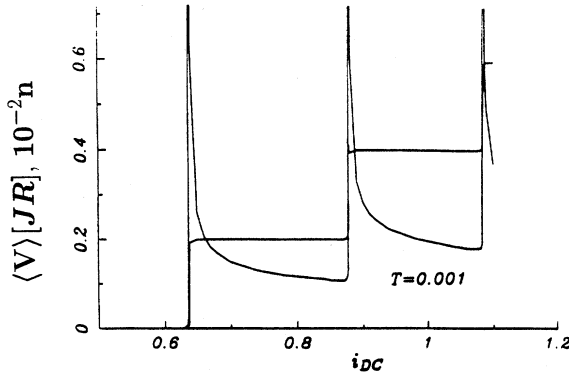


FIG. 4. A plot of the number of vortex-antivortex pairs ($\times 100$) per lattice plaquette, averaged over 40 000 snapshots (taken at different times) for each value of the current vs i_{dc} for $i_{dc}=0.5$, $\omega=0.2$, and $T=0.001$ in a 16×16 array.

fluctuations) at $T=0.001$ in units of $\hbar J/ek_g$. (For example, in these units the Kosterlitz-Thouless transition occurs at about $T_{KT}=0.45$.) The $(V-I)$ curves for the single junction and for the junctions in the $N \times N$ array are now rounded by the temperature fluctuations although the steps for the $N \times N$ array are less rounded than those for the single junction.

In the numerical simulations, in the array we can observe and count the antivortex-vortex pairs present at any given time. An example of a snapshot of the creation of an

antivortex-vortex pair in a 16×16 array is shown in Fig. 3. This numerical process was discussed in more detail in Cai *et al.*⁷ where it was observed that the vortices were created numerically by the random temperature (current) fluctuations. Essentially a hot fluctuation region acts momentarily as a local defect diverting the supercurrent around each side of it, with the resulting vortex and antivortex being created and depinned from the edge of this fluctuation. Using this technique it is easy to observe, for example, the antivortex-vortex pairs created at the Kosterlitz-Thouless transition.⁷ So here, these vortices were easily identified and counted by the computer where they were identified as singularities in the superconducting phase field. Specifically, we searched each square plaquette of nearest-neighbor sites for phase change of $\pm 2\pi$ as one transverses the sites around the plaquette. The results of this vortex count are shown in Fig. 4 superimposed upon the $(V-I)$ curve for the array, where the vertical axis is the number of vortices ($\times 100$) counted in the array averaged over 40 000 snapshots taken at each value of the bias current i_{dc} . The random samples were generated independently at each value of the current i_{dc} so the results at each value of i_{dc} are not correlated. From Fig. 4 it is clear that the peaks in the number of vortices in the array occur just at the risers of the Shapiro steps when the system is making the transition to the next harmonic. The vortex-number peaks have long tails on the high-current side. A four-parameter fit of the first peak to a power law of the form

$$n_v = a + b(i_{dc} - i_1)^{-x}$$

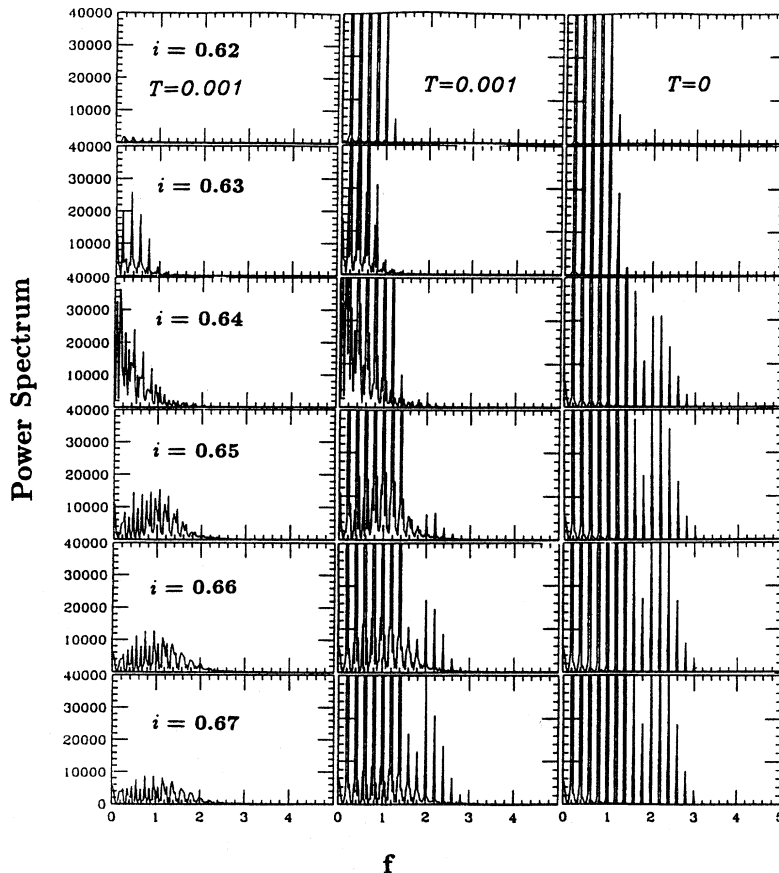


FIG. 5. The power spectrum (Fourier components of the voltage squared vs frequency) of a 5×5 RSJ array for $i_{dc}=0.62-0.67$. The peak in the number of vortices occur at the step riser at $i_{dc}=0.64$. The right-hand column is for $T=0$, the central column is $T=0.001$, and the left-hand column is also at $T=0.001$, but with the harmonic peaks removed.

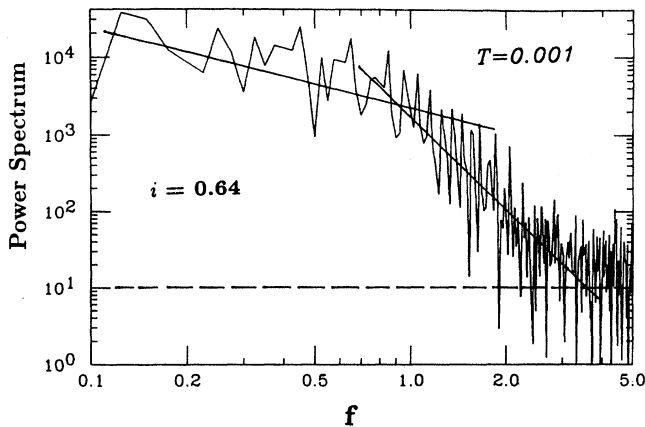


FIG. 6. The power spectrum of Fig. 5, for the case of the peak number of vortices, at $T=0.001$ and $i_{dc}=0.64$ redrawn as a log-log plot, with the harmonic peaks removed. The solid-state straight lines with slopes of -1 and -4 are merely guides to the eye.

gives $x=0.46 \pm 0.05$, $i_1 \equiv 0.639 \pm 0.001$, $b=0.0255$, and $a=0.0563$. So these upper tails are approximately square-root singularities.

It also seems that these vortex peaks are responsible for a substantial rise in the noise produced at the step risers. In Figs. 5 and 6 we show the power spectrum as one goes through the first peak in the vortex numbers. For Fig. 5, right-hand column, we show the power spectrum at $T=0$ for the six values of the bias current in the range $i_{dc}=0.62-0.67$. Clearly there are only the harmonics produced at $T=0$ at multiples of the applied frequency $\omega=0.2$. When the temperature is raised to $T=0.001$, center column, there is a reduction in the amplitudes of the harmonics coupled with a dramatic increase in the noise produced as one passes through the peak in the number of vortices at about $i_{dc}=0.64$. It is an easy matter to subtract out the harmonics which occur at $\omega=0.2n$ and one is left with the noise spectrum shown in the left-hand. The power spectrum is replotted at the vortex peak $i_{dc}=0.64$ in a log-log plot in Fig. 6. The background noise in these units for $T=0.001$ is about 10^1 so the noise power at its peak increases by about 3-4 orders of magnitude over this value. The suggestive straight lines drawn in Fig. 6 have slopes of -1 and -4 . The region of -1 slope may represent $1/f$ -noise, although we were able to observe this behavior only over a rather small frequency

range. It may also be that thermal-fluctuation-driven vortex-pair creation is an important contributor to the anomalous noise temperature seen experimentally in some single Josephson junctions.^{1,2} It would be useful to have similar measurements on real RSJ arrays to see the effect simulated here.

Finally, as one test of the variation of the supercurrent induced by the ac field predicted by the single junction calculation¹ we attempted to calculate the single-time voltage-voltage correlation function within a 19×19 sample. The results had rather large fluctuations in the data but nevertheless the correlation function on the step riser died much more rapidly with distance and there were some indications that the correlation function was changing from a power-law behavior within the superconducting phases on the steps to an exponential decay on the riser which would be characteristic of the normal state. It would seem that, perhaps the system is going normal briefly on the risers of the Shapiro steps.

In conclusion, we believe that we have seen evidence for a large increase in the number of unbound vortex pairs on the Shapiro-step risers as the bias current passes through the critical values. This is like a kind of Kosterlitz-Thouless transition in the sense that the vortex pairs created on and bound to the edges of the thermal fluctuations depin when the locked state becomes unstable on the Shapiro-step risers. Nevertheless, the cooperative effects of the coupled nonlinear Josephson junctions at the Shapiro-step risers in this array keep the fluctuations sufficiently low compared to those for a single junction that the step rounding is reduced. It would be interesting to see experimental verification of the noise results seen here and analytic calculations that would study the transition phenomena between the Shapiro steps.

We are grateful to the CAIP Center at Rutgers and to the NCUBE Corporation for access to their NCUBE Computer System, and to Z. Yu of NCUBE for assistance with the parallel computer programming. We gratefully acknowledge the vital grant of computer time at the NSF Pittsburgh Superconducting Center without which this project could not have been done. We thank for their hospitality the Department of Physics and Astronomy of Michigan State University where the authors were visitors and P.L.L. thanks Theoretical Physics and New College, Oxford University for their hospitality where this work was completed. Finally, we should like to acknowledge useful conversations with Philip Duxbury, Chris Lobb, and Richard Newrock regarding this calculation.

¹R. Y. Chiao, M. J. Feldman, D. W. Peterson, B. A. Tucker, and M. T. Levinson, in *Future Trends in Superconductive Electronics*, edited by B. S. Deaver, C. M. Falco, J. H. Harris, and S. A. Wolf, AIP Conf. Proc. No. 44 (AIP, New York, 1978), p. 259.

²Y. Taur and P. L. Richards, *J. Appl. Phys.* **48**, 1321 (1977).

³B. A. Huberman, J. P. Crutchfield, and N. H. Packard, *Appl. Phys. Lett.* **37**, 750 (1980).

⁴R. L. Kautz, *J. Appl. Phys.* **52**, 6241 (1981).

⁵N. F. Pedersen and A. Davidson, *Appl. Phys. Lett.* **39**, 830 (1981).

⁶W. C. Stewart, *Appl. Phys. Lett.* **12**, 277 (1968); D. E. McCumber, *J. Appl. Phys.* **39**, 3113 (1968).

⁷Y. Cai, P. L. Leath, and Z. Yu, *Phys. Rev. B* **49**, 4015 (1994).

⁸V. Ambegaokar and B. I. Halperin, *Phys. Rev. Lett.* **22**, 1364 (1969).